CHALMERS
UNIVERSITY OF TECHNOLOGY

Belief Propagation-based Target Handover in Distributed Integrated Sensing and Communication

Belief Propagation-based Target Handover in Distributed Integrated Sensing and Communication

Liping Bai, Yu Ge, Henk Wymeersch
Chalmers University of Technology, Gothenburg, Sweden

***Abstract*—Distributed integrated sensing and communication (DISAC) systems are key enablers for 6G networks, offering the capability to jointly track multiple targets using spatially distributed base stations (BSs). A fundamental challenge in DISAC is the seamless and efficient handover of target tracks between BSs with partially overlapping fields of view, especially in dense and dynamic environments. In this paper, we propose a novel target handover framework based on belief propagation (BP) for multi-target tracking in DISAC systems. By representing the probabilistic data association and tracking problem through a factor graph, the proposed method enables efficient marginal inference with reduced computational complexity. Our framework introduces a principled handover criterion and message-passing strategy that minimizes inter-BS communication while maintaining tracking continuity and accuracy. We demonstrate that the proposed handover procedure achieves performance comparable to centralized processing, yet significantly reduces data exchange and processing overhead. Extensive simulations validate the robustness of the approach in urban tracking scenarios with closely spaced targets.**

***Index Terms*—6G, DISAC, tracking, trajectory, target handover, belief propagation.**

I. Introduction

The integrated sensing and communications (ISAC) paradigm leverages existing communication infrastructure for sensing and localization, either as a standalone service or as an auxiliary function to support communication [1]. In urban environments, scalability challenges in communication systems emerge from the high density of users. A common remedy is to partition the service area into cells [2], each managed by a single base station (BS), with users handed over from one cell to another [3]. Extending this divide-and-conquer strategy to ISAC results in the concept of distributed integrated sensing and communications (DISAC) [4], [5].

The DISAC setup leads naturally to the multi-sensor multi-target tracking (MTT) problem, which involves tracking multiple targets using multiple homogeneous sensors (BSs, in the context of DISAC), each with limited field of view (FoV) [6]. MTT jointly estimates the number and states of a time-varying set of targets from noisy measurements, while addressing measurement origin uncertainty, missed detections, false alarms, and an unknown target count. Centralized processing of multi-sensor MTT can significantly outperform single-sensor approaches [7]–[10], but distributed multi-sensor MTT without a fusion center introduces further challenges [11].

This work has been supported by the Wallenberg Foundations through the Wallenberg AI, Autonomous Systems and Software Program. This work has been supported by the SNS JU project 6G-DISAC under the EU's Horizon Europe research and innovation Program under Grant Agreement No 101139130.

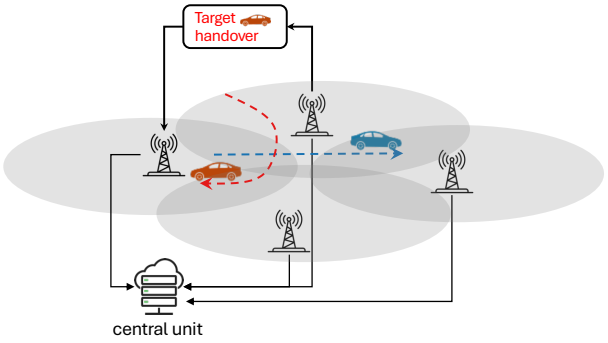

Fig. 1: Example of a DISAC scenario with a central unit. Four BSs are shown, with finite and overlapping FoVs. Target handover enables efficient tracking without needing to share raw data with the central unit.

Target handover, where tracking responsibility shifts from one sensor to another as targets move across FoVs, is an effective strategy to address these challenges [12].

Recent DISAC research has produced various target handover methods. A generalized framework for target mobility management, including dynamic sensing configuration handover, was presented in [13]. A primary BS handover within a virtual sensing cell (VSC)—defined as three neighbouring cells—as well as a handover mechanism between VSCs was proposed in [14]. In [15], a random finite set (RFS)-based handover method has been developed. It achieves excellent performance but has poor scalability due to the need to maintain numerous global association hypotheses. In the MTT context, RFS-based methods [16] are often contrasted with low-complexity belief propagation (BP)-based approaches, which scale linearly with the number of targets and measurements [17]. This motivates combining BP with target handover.

In this paper, we propose a novel BP-based handover mechanism for MTT in DISAC systems. Our specific contributions are as follows: *(i)* we introduce a new handover algorithm for BP-based multi-cell MTT, incorporating a principled message-passing criterion based on target belief states; *(ii)* we formulate the handover process using factor graphs, enabling compatibility with existing BP-MTT approaches while minimizing inter-BS communication; *(iii)* we systematically compare centralized, distributed, and handover tracking architectures, demonstrating that our approach matches the accuracy of centralized tracking at a fraction of the communication cost; and *(iv)* we release an open-source simulation framework to facilitate reproducibility and further exploration in the community. It is located at https://github.com/BaiLiping/BPTargetHandover.

II. System Model

In this section, we describe the kinematic state of the targets and the measurement model.

Target State Model: At discrete time k, each target i is represented by a kinematic state vector $\mathbf{x}_k^i$ that comprises its position and velocity. The state transition density is given by $f(\mathbf{x}_k^i|\mathbf{x}_{k-1}^i)$. In this paper, we assume the constant velocity and stochastic acceleration kinematic model [18], $\mathbf{x}_k^i = \mathbf{F}\mathbf{x}_{k-1}^i + \mathbf{v}_{k-1}^i$, where $\mathbf{F}$ is the state transition matrix and $\mathbf{v}_k^i$ the additive zero-mean Gaussian process noise with covariance matrix $\mathbf{Q}$.

Measurement Model: In the DISAC system, there are $n_s > 1$ BSs with known positions and partially overlapping FoVs. At time k, a set with n_m measurements $\mathbf{Z}_{k,s} = [\mathbf{z}_{k,s}^1, \ldots, \mathbf{z}_{k,s}^{n_m}]$, is obtained by the BS s. Each element in the set can originate from a target or clutter, where clutter is modeled by Poisson point process (PPP) with intensity $c(\mathbf{z})$. We introduce a detection probability function on the kinematic state $p_d^s(\mathbf{x}_k^i) \in [0,1]$. To model the FoV of BS s, we specify the following: if $\mathbf{x}_k^i \in \mathrm{FoV}_s$, then $p_d^s(\mathbf{x}_k^i) > 0$, and $p_d^s(\mathbf{x}_k^i) = 0$ otherwise. When a measurement $\mathbf{z}_{k,s}^m$ originates from target i, the measurement $\mathbf{z}_{k,s}^m$ is modeled as $\mathbf{z}_{k,s}^m = \mathbf{h}_s\left(\mathbf{x}_k^i\right) + \mathbf{w}_{k,s}^i$, where $\mathbf{h}_s(\cdot)$ is a nonlinear measurement function for BS s, and $\mathbf{w}_{k,s}^i$ is the additive zero mean Gaussian measurement noise with covariance matrix $\mathbf{R}$. Measurement includes tuples comprising the time of arrival (ToA) and angle of arrival (AoA) of channel paths [19], obtained through standard channel parameter estimation methods [20]. The equivalent likelihood function for measurement originating from a known target is: $f(\mathbf{z}_{k,s}^m|\mathbf{x}_k^i) = \mathcal{N}(\mathbf{z}_{k,s}^m; \mathbf{h}_s(\mathbf{x}_k^i), \mathbf{R})$.

III. BP-Based Multi-Sensor Multi-Target Tracking

To introduce BP-based MTT in a DISAC setup, we first briefly introduce factor graphs and the sum-of-product algorithm. Then, we discuss the case of a single-base-station BP-MTT. Finally, we explain centralized and distributed processing in the context of multiple-base-station BP-MTT.

A. Factor Graph and BP Basics

Factor graphs convey the computational structure of a joint probability density function (pdf) $f(x_1, \ldots, x_N)$ and are widely used for marginal posterior computations in robotics, communication, sensing, and machine learning [21]. In a factor graph, factors (usually depicted as squares) and variables (traditionally shown as circles) are connected when a function takes that variable as input. BP is a message passing method on a factor graph, whereby messages (functions) are computed and passed between factors and variables, which provides an efficient way to determine the marginals (also called the beliefs) $f(x_i)$, $i \in \{1, \ldots, N\}$.

B. Single BS MTT

We first consider the case of a single BS. We will introduce an augmented state to capture the unknown number of targets. Then we detail the prior, the likelihood, the factorization of the joint density, and the beliefs, largely based on [17, Sections IV and VIII]. Our focus will be on one time step (from $k-1$ to k), to simplify the notation, at the cost of some mathematical rigour.

1) Augmented States: To model the unknown and time-varying number of targets, we augment the kinematic state $\mathbf{x}_k^j$ with an auxiliary binary variable r_k^j, where $r_k^j = 1$ indicates the existence of the potential target (PT) and $r_k^j = 0$ otherwise. The augmented state of a PT is denoted by $\mathbf{y}_k^j = [\mathbf{x}_k^j, r_k^j]$. We distinguish between *new PTs* and *legacy PTs*, where every measurement is treated as an initial detection of a new PT, and these new PTs become legacy PTs in subsequent time steps. We denote the augmented state for new PT by $\overline{\mathbf{y}}_k$, and the augmented state for legacy PT by $\underline{\mathbf{y}}_k$. We denote the vector for all PTs by $\mathbf{Y}_k$, with $\mathbf{Y}_k = [\underline{\mathbf{Y}}_k, \overline{\mathbf{Y}}_k]$.

2) Prediction and Prior: We denote the posterior (or the belief) of the jth PT at time $k-1$ by $f(\underline{\mathbf{y}}_{k-1}^j)$. Each of the PTs at time $k-1$ corresponds to a legacy PT at time k. The state transition density for the jth legacy PT is

$$f(\underline{\mathbf{y}}_k^j|\underline{\mathbf{y}}_{k-1}^j) = \begin{cases} f_d(\underline{\mathbf{x}}_k^j) & \underline{r}_k^j = 0, \underline{r}_{k-1}^j = 0, \\ 0 & \underline{r}_k^j = 1, \underline{r}_{k-1}^j = 0, \\ (1 - p_s(\underline{\mathbf{x}}_{k-1}^j))\, f_d(\underline{\mathbf{x}}_k^j) & \underline{r}_k^j = 0, \underline{r}_{k-1}^j = 1, \\ p_s(\underline{\mathbf{x}}_{k-1}^j)\, f(\underline{\mathbf{x}}_k^j|\underline{\mathbf{x}}_{k-1}^j) & \underline{r}_k^j = 1, \underline{r}_{k-1}^j = 1, \end{cases} \tag{1}$$

where $p_s(\underline{\mathbf{x}}_{k-1}^j)$ is the survival probability of the PT and $f_d(\underline{\mathbf{x}}_k^j)$ is a dummy distribution (in the sense of being an arbitrary placeholder, that will be marginalized out when computing the beliefs). From the posterior of previous step $f(\underline{\mathbf{y}}_{k-1}^j)$ and the transition density $f(\underline{\mathbf{y}}_k^j|\underline{\mathbf{y}}_{k-1}^j)$, we can derive the prior pdf for the jth legacy PT at time k as $f(\underline{\mathbf{y}}_k^j) = \int f(\underline{\mathbf{y}}_k^j|\underline{\mathbf{y}}_{k-1}^j) f(\underline{\mathbf{y}}_{k-1}^j) \mathrm{d}\underline{\mathbf{y}}_{k-1}^j$.

The prior for the mth new PT is set to be $f_n(\overline{\mathbf{x}}_k^m)$, which in this paper is heuristically determined from the mth measurement $\mathbf{z}_k^m$.

3) Likelihood: To account for the unknown association between measurements and targets, we introduce two sets of discrete association variables: track-oriented association variables $\mathbf{a}_k$ and measurement-oriented association variables $\mathbf{b}_k$. Specifically, $a_k^j = m$ indicates that the jth PT is associated with measurement m (while $a_k^j = 0$ indicates that the jth PT is not detected), and $b_k^m = j$ indicates that measurement m is associated with jth PT (while $b_k^m = 0$ indicates that measurement m is associated with the new PT). To ensure that $\mathbf{a}_k$ and $\mathbf{b}_k$ are mutually consistent, there is a constraint $\Psi(\mathbf{a}_k, \mathbf{b}_k) \in \{0,1\}$. The binary compatibility function $\Psi(\cdot)$ can be factorized [17, Eq. (21)], which makes it computationally efficient in the factor graph representation and the associated BP.

We now introduce two so-called *pseudo-likelihood* functions for each legacy PT (denoted by $q(\cdot)$ for the jth legacy PT) and for each new PT (denoted by $v(\cdot)$ for the mth new PT).

These are defined as

$$q(\underline{\mathbf{x}}_k^j, \underline{r}_k^j, a_k^j; \mathbf{Z}_k) = \begin{cases} \frac{p_d(\underline{\mathbf{x}}_k^j)}{c(\mathbf{z}_k^m)} f(\mathbf{z}_k^m|\underline{\mathbf{x}}_k^j) & a_k^j = m \neq 0, r_k^j = 1, \\ 1 - p_d(\underline{\mathbf{x}}_k^j) & a_k^j = 0, r_k^j = 1, \\ 0 & a_k^j \neq 0, r_k^j = 0, \\ 1 & a_k^j = 0, r_k^j = 0. \end{cases} \tag{2}$$

and

$$v(\overline{\mathbf{x}}_k^m, r_k^m, b_k^m; \mathbf{z}_k^m) \tag{3}$$
$$= \begin{cases} 0 & b_k^m \neq 0, r_k^j = 1, \\ \frac{\mu_n}{c(\mathbf{z}_k^m)} f_n(\overline{\mathbf{x}}_k^m) f(\mathbf{z}_k^m|\overline{\mathbf{x}}_k^m) & b_k^m = 0, r_k^j = 1, \\ f_d(\overline{\mathbf{x}}_k^m) & r_k^j = 0. \end{cases}$$

where $\mu_n \geq 0$ is the mean number of newborn targets, which is Poisson distributed. The clutter intensity $c(\mathbf{z})$ is the expected number of clutter in an infinitesimal region around $\mathbf{z}$, and $c(\mathbf{z}) = \mu_c f_c(\mathbf{z})$, where $f_c(\mathbf{z})$ is the clutter pdf.

4) Factorization: With the pseudo-likelihoods defined, we can factorize the joint pdf at time step k based on conditional indepence as

$$f(\mathbf{Y}_k, \mathbf{a}_k, \mathbf{b}_k, \mathbf{Z}_k) \tag{4}$$
$$\propto \Psi(\mathbf{a}_k, \mathbf{b}_k) \prod_{j=1}^{n_p} f(\underline{\mathbf{y}}_k^j) q(\underline{\mathbf{y}}_k^j, a_k^j; \mathbf{Z}_k) \prod_{m=1}^{n_m} v(\overline{\mathbf{y}}_k^m, b_k^m; \mathbf{z}_k^m),$$

The corresponding factorization is presented by the factor graph in Fig. 2. The Bayesian estimation process is expressed in the messages passed in the factor graph from Fig. 2. All the messages passed from the factor node to the variable node $\mathbf{y}_k^j$ will be a weighted combination of all the cases (associations). We refer the readers to [17] for the equations for each message.

5) Posterior and Beliefs: At time step k, the inputs to the factor graph are the beliefs from time $k-1$, as shown in Fig. 2. For the jth legacy PT, propagating its input beliefs through the loopy factor graph results in an approximated posterior density $f(\underline{\mathbf{y}}_k^j|\mathbf{Z}_k)$. From this approximated posterior, two updated beliefs at time k can be obtained: one over the target's kinematic state $\tilde{p}(\underline{\mathbf{x}}_k^j) = \sum_{\underline{r}_k^j} f(\underline{\mathbf{y}}_k^j|\mathbf{Z}_k)$ and one over its existence $\tilde{p}(\underline{r}_k^j) = \int f(\underline{\mathbf{y}}_k^j|\mathbf{Z}_k) \mathrm{d}\underline{\mathbf{x}}_k^j$. Analogous beliefs are computed for each new PT. The existence belief $\tilde{p}(r_k^j = 1)$, also known as the posterior existence probability, is used to manage the PTs: we declare the jth PT to exist if $\tilde{p}(r_k^j = 1) > P_{\mathrm{th}}$, and we prune that PT if $\tilde{p}(r_k^j = 1) < P_{\mathrm{prune}}$, where P_{th} and P_{prune} are predetermined thresholds for declaring a target exists and pruning, respectively.

C. Multi-BS MTT

Now, we extend our discussion from the single BS to MTT with $n_s > 1$ BPs. This is formally known as a multi-sensor MTT problem. Each BS s obtain a set with n_{m_s} measurements $\mathbf{Z}_{k,s}$. There are now two extreme strategies:

- *Distributed Processing:* Each BS operates independently and executes the BP-MTT process outlined in Section III-B. This means that when PTs leave the FoV of a BS, they are lost to that BS in the sense that no more measurements will be associated with it. In addition, if that target enters the FoV of another BS, its track must be initialized from scratch.
- *Centralized Processing:* In this case, there is a central unit (See Fig. 1) to which all BSs send their measurements. There are several ways to proceed [8]–[10], but we present a simple sequential approach. In this sequential approach, the BSs are ordered and the central unit processes the measurements from each BSs sequentially, thereby generating new PTs, to which the measurements from the subsequent BSs can be associated. Effectively, sequentially updating the state beliefs in a sequence of n_s BSs in one time is the equivalent of updating the state beliefs in n_s time in a distributed setup.

Example 1 (Fusion between two BSs)**.** *To illustrate the sequential processing approach in the context of BP-MTT, we discuss the procedure for one new target located within the overlapping FoV between BS1 and BS2. There are two measurements, $\mathbf{z}_{k,1}$ at BS1 and $\mathbf{z}_{k,2}$ at BS2, originating from the target: $\mathbf{z}_{k,1}$ is first used to initiate the new PT with posterior $f(\overline{\mathbf{y}}_k^1|\mathbf{z}_{k,1})$. Then $\mathbf{z}_{k,2}$ is used to update the posterior $f(\overline{\mathbf{y}}_k^1|\mathbf{z}_{k,1})$ to $f(\underline{\mathbf{y}}_k^1|\mathbf{z}_{k,1}, \mathbf{z}_{k,2})$.*

IV. BP-Based Target Handover

In this section, we introduce the proposed target handover mechanisms. By target handover, we mean sharing the target information from one BS to one or more BSs, without deleting any information at transmission. The handover should not interfere with the BP-MTT process and avoid double-counting of measurements. We will present two target handover approaches: (i) with measurements exchange that exploits the overlapping FoV of BSs to improve target state estimation while minimizing the information exchanged between BSs (illustrated in Fig. 2); (ii) without measurements exchange in order to highlight the benefits of sharing measurements in the numerical experiments.

We focus on a single pair of BSs for notational clarity, though the methods extend to any configuration. We denote the BS initiating the handover as BS-Tx (index s_t) and the BS receiving the information as BS-Rx (index s_r). We assume parallel processing between the two BSs. That is, the handover priors are received by the BS-Rx before prediction steps at time k, and the handover measurements are received by the BS-Tx before the updating steps at time k.

A. Operation at the Transmitting BS (BS-Tx)

From BS-Tx, the handover process requires keeping track of several additional variables, as described below:

1) BS-Tx runs BP as described in Section III-B. Hence, the target handover algorithm does not interrupt the BP-MTT process at BS-Tx. As a side-effect of running BP, we obtain the marginal association probabilities $f^{(s_t)}(a_k^j|\mathbf{Z}_k)$. We can then obtain the index of the most likely associated measurement for the jth PT, denoted

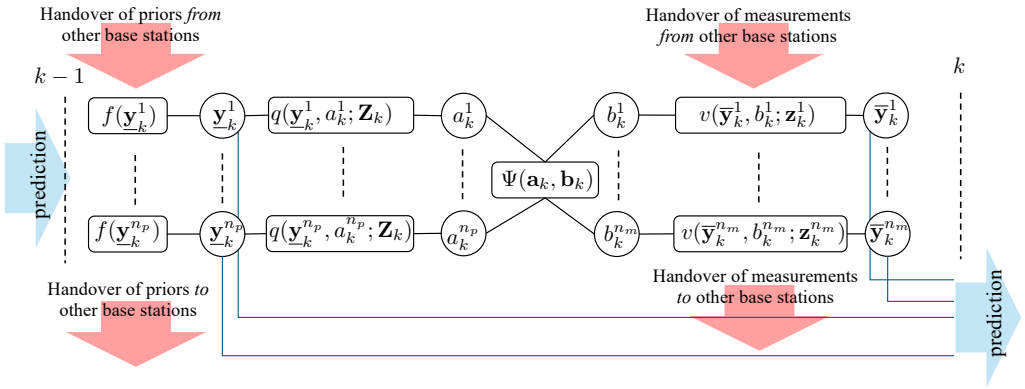

Fig. 2: Factor graph representation of $f(\mathbf{Y}_k, \mathbf{a}_k, \mathbf{b}_k, \mathbf{Z}_k)$. The prediction step can also be expressed as part of the factor graph, but is not shown for simplicity of the exposition. Handover of priors and measurements is shown in red.

$m^j = \arg\max_m f^{(s_t)}(a_k^j = m|\mathbf{Z}_k)$. If $m^j = 0$, the PT is most likely to be miss-detected and no measurement is handed over. The notation $f^{(s_t)}$ indicates that this density is computed at BS s_t.

2) For each PT j, we check if the target handover criterion $h_c^j \in \{0, 1\}$ is met:

$$h_c^j = \mathbb{I}\{f^{(s_t)}(\underline{r}_k^j = 1) > P_{\text{th}}\} \times \int p_d^{(s_r)}(\underline{\mathbf{x}}_k^j)\, f^{(s_t)}(\underline{\mathbf{x}}_k^j)\, \mathrm{d}\underline{\mathbf{x}}_k^j > \Gamma, \tag{5}$$

where $f^{(s_t)}(\underline{\mathbf{x}}_k^j)$ is the marginal of the prior $f^{(s_t)}(\underline{\mathbf{y}}_k^j)$ over the kinematic state and $f^{(s_t)}(\underline{r}_k^j)$ is the marginal of the prior over existence; $\mathbb{I}\{\mathsf{P}\}$ is an indicator function valued 1 if P is true and 0 otherwise; $p_d^{(s_r)}(\underline{\mathbf{x}}_k^j)$ is the BS-Rx detection probability; Γ a predefined handover threshold.

3) PTs for which $h_c^j = 1$ and $m^j > 0$ are potential candidates for handover. To avoid repeated handovers of the same PT, each PT j is assigned a unique local label, say $L_j^{(s_t)} \in \mathbb{N}$, at BS-Tx. Once a target has been handed over for the first time, its label is appended to a local list $\mathcal{T}^{(s_t \to s_r)}$, where the subscript $(s_t \to s_r)$ indicates it is a list for handover labels from BS-Tx to BS-Rx.

4) The actual handover now proceeds. If $h_c^j = 1$ and $L_j^{(s_t)} \notin \mathcal{T}^{(s_t \to s_r)}$, this is the first time we hand over this target from BS-Tx to BS-Rx. We hand over the prior $f^{(s_t)}(\underline{\mathbf{y}}_k^j)$ and append $L_j^{(s_t)}$ to $\mathcal{T}^{(s_t \to s_r)}$. If $m^j \neq 0$, we also hand over $\mathbf{z}_k^{m_j}$ from BS-Tx to BS-Rx. On the other hand, if $h_c^j = 1$ and $L_j^{(s_t)} \in \mathcal{T}^{(s_t \to s_r)}$, then this target was handed over before and we should not hand over the prior, to avoid double counting of information. Only the measurement $\mathbf{z}_k^{m_j}$ is handed over, provided $m^j \neq 0$.

5) When a PT is pruned or leaves the FoV of BS-Tx, its label is removed from $\mathcal{T}^{(s_t \to s_r)}$.

The target handover variant without measurements follows the same steps, but never hands over the measurements.

B. Operation at the Receiving BS (BS-Rx)

Now we describe the target handover algorithm for BS-Rx. At time k, BS-Rx receives from BS-Tx a number of priors of PTs and a number of measurements. BS-Rx now incorporates this information as follows:

1) The received priors are appended to the local priors, effectively increasing the number of legacy PTs in the factor graph. This leads to an increased complexity due to the larger number of legacy PTs, but allows BS-Rx to quickly detect new PTs entering its FoV. Each received PTs is associated with a unique local label $L^{(s_r)}$, which is added to the local list $\mathcal{R}^{(s_r \leftarrow s_t)}$ to prevent duplicate handovers.
2) BS-Rx runs BP sequentially (as detailed in Section III-C), first its local measurements and then using the handed over received measurements from other BSs.
3) When a PT is pruned or leaves the FoV of BS-Rx, its label is removed from $\mathcal{R}^{(s_r \leftarrow s_t)}$.

The target handover without measurements for BS-Rx follows the same steps, omitting only the measurement-related sequential processing.

Remark 1. *All BSs are acting as BS-Tx and BS-Rx at each time step and maintain transmission and reception lists with respect to all neighboring BSs and also share the information related to the FoV, in the form of the spatial detection probability. It is also important to highlight that priors are handed over before BP update at time step k, while measurements are handed over after BP update at time step k.*

V. Numerical Results

We evaluate the proposed BP-based handover approach in a simulated DISAC scenario and compare to distributed and centralized baselines.

A. Scenario

Two BSs, denoted BS1 and BS2, are located at $[0\text{m}, 0\text{m}]$ and $[150\text{m}, 0\text{m}]$, respectively. Each BS has a circular FoV with radius 120 m centered at its position. Two moving targets traverse the combined surveillance region; their start and end positions, as well as their trajectories, are shown in Fig. 3. Simulations considered a sampling interval of 1 s over 100 time steps. From about 35 s to 70 s, there are on average two targets. The target handover is initiated around 25 s to 35 s. Between time steps 47 and 52, the two targets pass close to

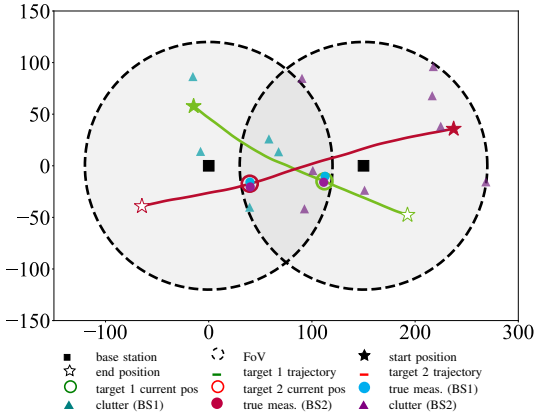

Fig. 3: Simulation scenario with 2 BSs and two targets. Axes are in meters.

one another, as illustrated in Fig. 3. For data generation, we use the following settings for both BSs: $p_d(\mathbf{x}) = 1$ when $\mathbf{x} \in$ FoV and $p_d(\mathbf{x}) = 0$ otherwise; a constant survival probability $p_s(\mathbf{x}) = 0.99$; to set $\mathbf{Q}$, we use the model [18, eq. 6.3.2-4] with process noise standard deviation $\sigma_v = 0.05$ m on both x and y coordinates; measurement noise covariance $\mathbf{R} = \text{diag}(\sigma_r^2, \sigma_\theta^2)$ where $\sigma_r = 1$ m and $\sigma_\theta = 1^\circ$ for ToA (converted to distance) and AoA, respectively. The value of μ_c is set to be 5 and the clutter is distributed uniformly over the respective FoV.

B. BP-MTT Implementation

We implemented the BP-MTT methods in both particle filter and extended Kalman filter (EKF), and they can be found in the provided open source code. We will discuss the particle filter and display its results. All the parameters are set to be the same for both BSs. For the particle filter implementation, the number of particles is $10,000$. The threshold for pruning is $P_{\text{prune}} = 10^{-5}$, and the detection threshold is set to $P_{\text{th}} = 0.5$. The handover criterion Γ is 0.5. The μ_n is set to be 0.01, and the new target is uniformly distributed in the FoV. Different from the generative model, we set $p_d(\mathbf{x}) = 0.9$ when $\mathbf{x}$ is within the FoVs and $p_d(\mathbf{x}) = 0$ otherwise. In addition, $p_s(\mathbf{x})$, σ_θ, σ_r, σ_r, μ_c are all set to be identical to that of the data generation process.

We implemented four algorithms for comparison: distributed processing (from Section III-B), centralized processing (from Section III-C), and the proposed target handover with and without measurements (from Section IV). For each of the four algorithms, we ran 100 Monte Carlo (MC) trials and evaluated performance via the generalized optimal subpattern assignment (GOSPA) [22] metric.[1]

C. Results and Discussion

The scores for both BS1 and BS2 are evaluated with estimates and true tracks within their respective FoV. We present only the results for BS1 (results for BS2 are available in the code).

[1]The overall GOSPA score consists of three components: missed-detection score (no detection can be associated with the true track), false alarm score (detection when there is no track), and the localization score (Euclidean distance between the true track and the closest assigned estimation). The lower the overall GOSPA score, the better the performance of the proposed methods. The detailed GOSPA implementation and parameters are provided in the simulation code.

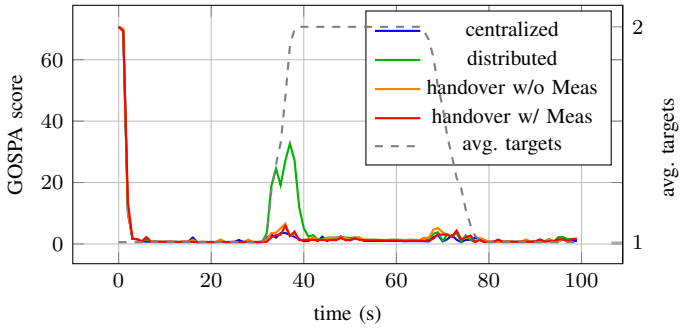

Fig. 4: GOSPA score for BS1.

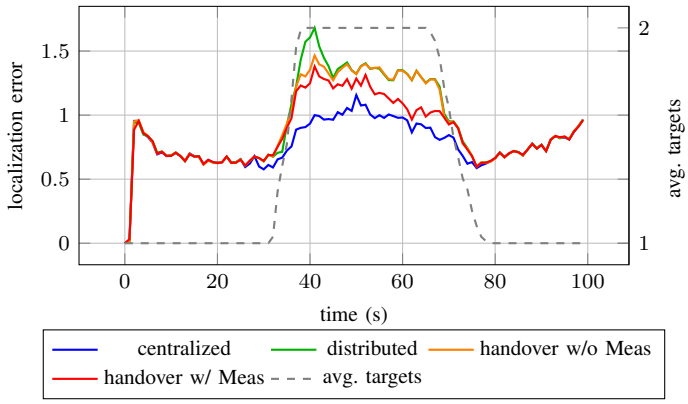

Fig. 5: Localization error for BS1.

The overall GOSPA score for BS1 is shown in Fig. 4. The proposed target handover with measurements algorithm achieves an overall GOSPA score comparable to that of the centralized approach, thanks largely to its reduction in missed-detection error. Since the missed-detection error dominates the GOSPA decomposition, the overall GOSPA curve closely mirrors the missed-detection curve. In the following paragraphs, we will analyse each of the three contributors to the GOSPA score—localization error, missed-detection error, and false-alarm error—in detail.

The localization error component in the GOSPA for BS1, shown in Fig. 5, demonstrates that within the overlapping FoV, the centralized algorithm achieves the lowest error, followed by the target handover with measurements algorithm. The handover without measurements approach yields only a slight error reduction at the start of the handover before its performance converges to that of the fully distributed method. This underscores the benefit of exchanging measurements during handover. All algorithms exhibit increased localization errors in the overlap region, where the reduced separation between targets makes data association more challenging.

The missed-detection error component for BS1 is shown in Fig. 6. All algorithms exhibit elevated missed-detection errors in the initial frames, since it takes several steps for the posterior existence probability to exceed the detection threshold P_{th}. In the fully distributed case, a pronounced spike in missed detections occurs when the target first moves into the FoV of BS1, because a new track must be initiated lo-

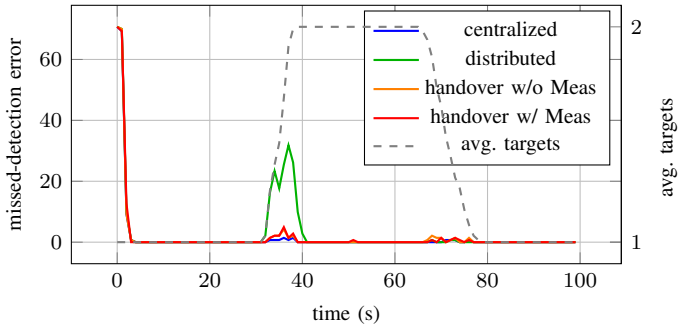

Fig. 6: missed-detection error for BS1.

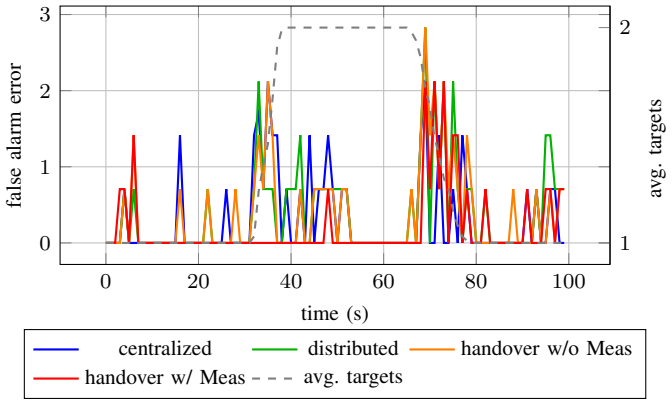

Fig. 7: False alarms error for BS1.

cally. Both the target handover without measurements and the target handover with measurements schemes achieve missed-detection performance comparable to that of the centralized algorithm.

The false alarm error component for BS1 is presented in Fig. 7. We observe elevated false alarm rates at the boundary of the overlapping FoV for both the target handover with measurements and the target handover without measurements schemes. The timing of the target handover is determined by the handover threshold Γ. Increasing Γ would likely decrease false alarm errors at the cost of higher missed-detection errors. Within the overlapping FoV, the target handover with measurements approach achieves significantly fewer false alarms than the target handover without measurements case.

VI. Conclusions

We have proposed a novel belief-propagation-based target handover procedure for MTT in DISAC systems. Our approach addresses the need for scalable, decentralized tracking in scenarios where targets move across overlapping fields of view covered by spatially distributed base stations. By leveraging factor graph representations and message-passing principles, the proposed method enables efficient target handover with limited communication overhead. Through detailed simulations, we have shown that the proposed handover mechanism achieves tracking performance comparable to centralized processing, while avoiding its high bandwidth and computational requirements. The algorithm maintains track continuity across base stations and is well-suited for dense urban environments where scalability and low latency are critical. Future work will focus on extending the handover procedure to support more complex and dynamic sensing configurations and real-time operation over heterogeneous networks. In addition, integrating this method into standardized communication frameworks for ISAC will be an important step toward practical deployment in 6G systems.

References

[1] N. González-Prelcic, *et al.*, "The integrated sensing and communication revolution for 6G: Vision, techniques, and applications," *Proceedings of the IEEE*, vol. 112, no. 7, pp. 676–723, 2024.

[2] A. Taufique, *et al.*, "Planning wireless cellular networks of future: Outlook, challenges and opportunities," *IEEE Access*, vol. 5, pp. 4821–4845, 2017.

[3] R. Fantacci, "Performance evaluation of prioritized handoff schemes in mobile cellular networks," *IEEE Transactions on Vehicular Technology*, vol. 49, no. 2, pp. 485–493, 2000.

[4] E. C. Strinati, *et al.*, "Toward distributed and intelligent integrated sensing and communications for 6G networks," *IEEE Wireless Communications*, vol. 32, no. 1, pp. 60–67, 2025.

[5] K. Meng, *et al.*, "Cooperative ISAC networks: Opportunities and challenges," *IEEE Wireless Communications*, pp. 1–8, 2024.

[6] N. F. Sandell *et al.*, "Distributed data association for multi-target tracking in sensor networks," in *2008 47th IEEE Conference on Decision and Control*. IEEE, 2008, pp. 1085–1090.

[7] A. K. Gostar, *et al.*, "Centralized cooperative sensor fusion for dynamic sensor network with limited field-of-view via labeled multi-bernoulli filter," *IEEE Transactions on Signal Processing*, vol. 69, pp. 878–891, 2020.

[8] Y. Bar-Shalom *et al.*, *Multitarget-multisensor tracking: principles and techniques*. YBS publishing Storrs, CT, 1995, vol. 19.

[9] B.-N. Vo, *et al.*, "Multi-Sensor Multi-Object Tracking with the Generalized Labeled Multi-Bernoulli Filter," *IEEE Transactions on Signal Processing*, vol. 67, no. 23, pp. 5952–5967, 2019.

[10] W. Zhou, *et al.*, "A scalable method for group target tracking using multisensor with limited field of views," *Journal of Radars*, vol. 12, no. 2, pp. 215–226, 2023.

[11] H. Van Nguyen, *et al.*, "Distributed multi-object tracking under limited field of view sensors," *IEEE Transactions on Signal Processing*, vol. 69, pp. 5329–5344, 2021.

[12] J. Kim, *et al.*, "Optimal target assignment with seamless handovers for networked radars," *Sensors*, vol. 19, no. 20, p. 4555, 2019.

[13] Y. S. Ribeiro, *et al.*, "Mobility management in integrated sensing and communications networks," *arXiv preprint arXiv:2501.08159*, 2025.

[14] Y. Feng, *et al.*, "Networked ISAC based UAV tracking and handover towards low-altitude economy," *IEEE Transactions on Wireless Communications*, pp. 1–1, 2025.

[15] Y. Ge, *et al.*, "Target handover in distributed integrated sensing and communication," *arXiv preprint arXiv:2411.01871*, 2024.

[16] Á. F. García-Fernández, *et al.*, "Poisson multi-Bernoulli mixture filter: Direct derivation and implementation," *IEEE Transactions on Aerospace and Electronic Systems*, vol. 54, no. 4, pp. 1883–1901, 2018.

[17] F. Meyer, *et al.*, "Message passing algorithms for scalable multitarget tracking," *Proceedings of the IEEE*, vol. 106, no. 2, pp. 221–259, 2018.

[18] Y. Bar-Shalom, *et al.*, *Estimation with applications to tracking and navigation: theory algorithms and software*. John Wiley & Sons, 2004.

[19] K. Venugopal, *et al.*, "Channel estimation for hybrid architecture-based wideband millimeter wave systems," *IEEE Journal on Selected Areas in Communications*, vol. 35, no. 9, pp. 1996–2009, 2017.

[20] F. Jiang, *et al.*, "Beamspace multidimensional ESPRIT approaches for simultaneous localization and communications," *arXiv preprint arXiv:2111.07450*, 2021.

[21] F. Kschischang, *et al.*, "Factor graphs and the sum-product algorithm," *IEEE Transactions on Information Theory*, vol. 47, no. 2, pp. 498–519, 2001.

[22] A. S. Rahmathullah, *et al.*, "Generalized optimal sub-pattern assignment metric," in *2017 20th International Conference on Information Fusion (Fusion)*, 2017, pp. 1–8.